ELSEVIER

PII: S0032-3861(97)10203-8

Polymer Vol. 39 No. 22, pp. 5515–5521, 1998

0032-3861/98/$ - see front matter

Crystallization behaviour of poly(L-lactide)

Tadakazu Miyata[a,*] and Toru Masuko[b]

[a]*Oji Paper Co., Ltd, Advanced Technology Research Laboratory, 1-10-6, Shinonome, Koto-ku, Tokyo 135, Japan*

[b]*Faculty of Engineering, Yamagata University, 4-3-16, Jonan, Yonezawa, Yamagata 992, Japan*

(Received 18 September 1997; accepted 6 October 1997)

The crystallization characteristics of poly(L-lactide) (PLLA) films of different molecular weights have been studied by differential scanning calorimetry, optical microscopy and a depolarized-light intensity (d.l.i.) method. In non-isothermal crystallization modes from the isotropic melt, the crystallinity of PLLA films increased remarkably with a decrease in the cooling rate, accompanied by a kind of annealing effect. Overall isothermal crystallization rates of the polymer determined by d.l.i. in the range from 90°C to 140°C indicated the maximum value at 105°C. This temperature is lower than that (120°C) at which the maximum spherullite growth rate is observed. The PLLA polymer exhibited an Avrami exponent $n = 4$ in the isothermal d.l.i. experiments over the whole temperature range examined. Molecular parameters governing the isothermal crystallization behaviour have been estimated by the application of secondary nucleation theory.

(Keywords: poly(L-lactide); morphology; crystallization kinetics)

INTRODUCTION

In recent years, much attention has been focused on biodegradable and biocompatible polymers, particularly from an ecological viewpoint. They are expected to be utilized for surgical implant materials and drug delivery systems. The mechanical properties and degradation rates of biodegradable polymers, in general, depend on their morphology or crystallinity as well as on their chemical structures.

Poly(L-lactide) (PLLA) is one biodegradable, synthetic polymer of great interest. Many publications concerning the degradation mechanism of PLLA both *in vitro* and *in vivo* have been published[1–11]. In parallel with degradative investigations, several studies on the solid state of PLLA have been carried out by X-ray diffraction (XRD) and conformational analysis of the molecular chain[12–15]. In recent X-ray works, it is proposed that the α-form of the PLLA crystal is composed of 10/3 helical chains[13–15]. Furthermore, Eling *et al.*[7] were the first to find another crystal modification (the β-form) which contains 3/1 helical chains of PLLA.

Examinations concerned with the crystallization behaviour of PLLA have also been published by several investigators. For example, Vasanthakumari and Pennings[16] reported the growth characteristics of PLLA spherulites as functions of undercooling and molecular weight, mainly by means of optical microscopy. Along with that report, Kishor and Vasanthakumari[17] examined the crystallization parameters for PLLA by means of a differential scanning calorimetry (d.s.c.) technique. However, the isothermal crystallization mechanism for PLLA seems not to have been examined sufficiently in those publications. The relationship between structural features and crystallization (or annealing) conditions under an isothermal or non-isothermal process is required from a fundamental viewpoint.

In our previous paper[18], the morphology and structural features of solution-grown crystals of PLLA were examined by transmission electron microscopy with the diffraction mode, wide-angle X-ray diffractometry and atomic force microscopy. In this study, we examine the crystallization characteristics of PLLA bulk films under various thermal conditions with respect to the change in crystallinity and spherulite morphology.

EXPERIMENTAL

Polymer synthesis

Well-purified L,L-lactide (Tokyo Kasei Kogyo Co., Ltd, Japan) was placed in evacuated tubes containing 0.03% (w/w) stannous octanoate (Sigma Chem. Corp., USA) and 0.01% (w/w) lauryl alcohol (Tokyo Kasei Kogyo Co., Ltd, Japan) as a catalyst activator and chain control agent[4]. Polymerization was carried out in the tube dipped into a silicone oil bath at 220°C for 5 min to 4 h. The solid polymer in the tube was dissolved in chloroform and then precipitated repeatedly from a large quantity of methanol at room temperature. The resultant polymer was white and fibrous in appearance. Molecular characterization results of the PLLA used in this work are listed in *Table 1*.

Film specimens

The PLLA polymer was sandwiched between two glass plates, heated to above its respective melting point (T_m) and then quenched into ice water. The quenched films were crystallized isothermally at various temperatures or subjected to non-isothermal crystallization at different cooling rates in a nitrogen atmosphere. For optical microscope observations, solution-cast films 10 μm thick were cast from a 1 wt% chloroform solution onto a glass plate in an air oven at 26°C, and then dried in a vacuum oven at 45°C.

* To whom correspondence should be addressed

Table 1 Characteristics of the PLLA used in this work

Infra-red absorption (cm^{-1})	C=O	ester	1760
	–O–	ester	1190
^{1}H nuclear magnetic resonance (ppm)	a	5.16	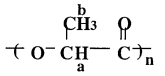
	b	1.58	
Gel permeation chromatography	A		$\overline{M}_w = 2.0 \times 10^5$
	B		$\overline{M}_w = 1.0 \times 10^5$
	C		$\overline{M}_w = 5.0 \times 10^4$

D.s.c. measurements

To examine the thermal properties of the PLLA films, a SEIKO DSC-200 calorimeter was utilized to obtain endothermic and exothermic changes in the range of 0–200°C at various heating (or cooling) rates in a nitrogen purge.

Optical microscopy

Spherulitic textures in the thin cast films (10 μm) were examined with an Olympus BH-2 polarizing microscope equipped with a video camera system. A Linkam THM-600 hot-stage device was also used in the range from 25°C to the temperature above the respective T_m of the PLLA samples.

Density measurements

The densities of the polymer films were determined at 25°C by using a density-gradient column filled with an aqueous $CaBr_2$ solution.

XRD measurements

Graphite-monochromatized Cu K_α radiation was employed for XRD experiments on a MAC Science M18XHF-SRA generator operated at 50 kV and 350 mA. XRD photographs and integral diffraction intensities for the specimens were taken at 23°C by means of an imaging plate system (DIP-220). Spacings of the reflection planes were measured, and correlated with those of standard cholesterol powder.

Depolarized-light intensity measurement

Isothermal crystallization measurements were carried out by use of a Kotaki MK-801 depolarized-light intensity (d.l.i.) apparatus[19] in the region from 90°C to 140°C. The electronic signals transformed from the measured d.l.i. were amplified and then recorded on a personal computer which accommodated an Avrami analysis software.

RESULTS AND DISCUSSION

Non-isothermal crystallization behaviour of the PLLA films

Figure 1 illustrates the heating/cooling d.s.c. traces at a rate of 10°C min^{-1} for the melt-cast PLLA film of specimen A ($\overline{M}_w = 2.0 \times 10^5$) mainly employed in this section. In the first heating run (curve 1) can be observed the glass transition (T_g) at ~55°C, a single exothermic peak at 115°C, and endothermic peaks (melting point, T_m) at 171°C. Upon cooling from 200°C, only a baseline change with T_g appears at 50°C (curve 2). When the specimen is subsequently heated, a similar thermogram to that in the first heating run is observed (curve 3). After two heating/cooling cycles, no change in the d.s.c. traces is observed at the same heating/cooling rate.

Interestingly, no exothermic peak can be observed in the first cooling run at 10°C min^{-1} (curve 2), and the exothermic enthalpy change at 115°C is close to the heat of fusion at 171°C (T_m) on the second heating run (curve 3).

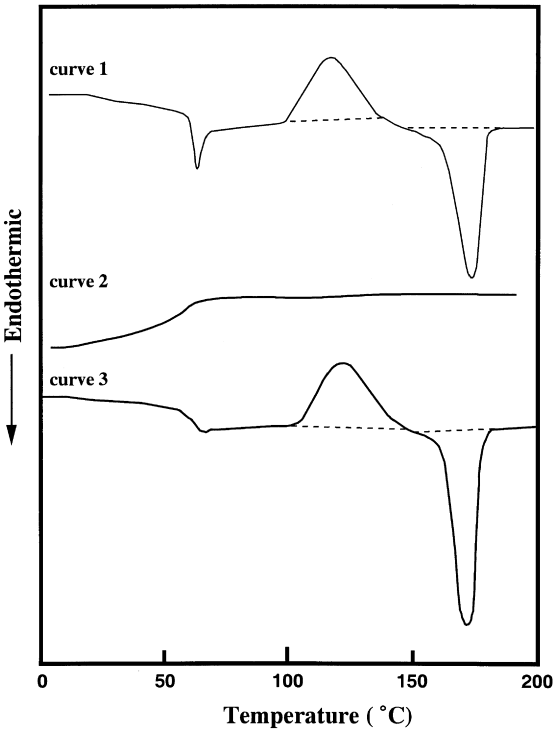

Figure 1 D.s.c. traces of the PLLA film in heating/cooling cycles

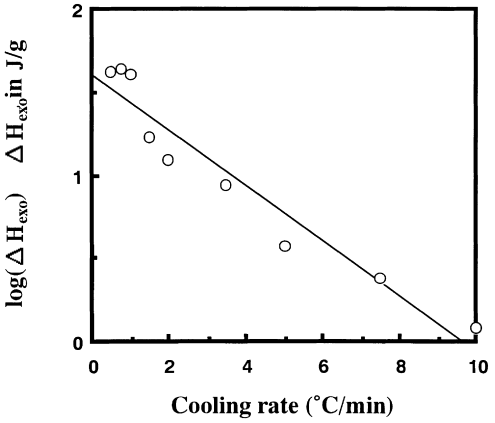

Figure 2 The logarithm of the exothermic enthalpy change as a function of the cooling rate from the isotropic melt

This implies that film specimens cooled from the isotropic melt a rate greater than 10°C min^{-1} remain amorphous. Thus, we examined first the crystallization behaviour of PLLA on the cooling process from the isotropic melt.

The quenched film was kept at 200°C for 10 min in the d.s.c. apparatus, and then cooled to room temperature at various cooling rates. *Figure 2* shows the logarithmic exothermic enthalpy change observed in the cooling process as a function of the cooling rate. The crystallinity of the PLLA film increases with decreasing cooling rate. In *Figure 2*, a fairly good linear relationship between both quantities is recognized. The exothermic enthalpy change obtained by extrapolating the cooling rate to 0°C min^{-1} in *Figure 2* is calculated to be almost 60 J g^{-1}. When these specimens were reheated at 10°C min^{-1} to 200°C, the d.s.c. traces obtained indicate that the baseline change at T_g, $\Delta C_p(T_g)$, decreases with reducing cooling rate. The $\Delta C_p(T_g)$ change finally disappears for the specimen cooled at 0.5°C min^{-1}. Also, the exothermic enthalpy change clearly increases with increasing cooling rates in the reheating process.

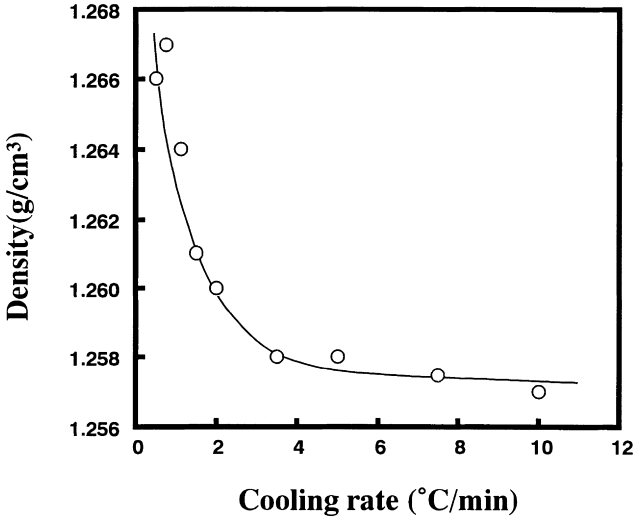

Figure 3 Changes in film density as a function of cooling rate from the isotropic melt

Figure 3 shows that the density of the annealed specimens increases with a decrease in the cooling rate. This tendency is similar to the relationship between the change in cooling rates and exothermic enthalpy changes in the cooling process. These results indicate that the crystallinity in the specimens depends on their annealing conditions, being especially influenced by slow cooling rates.

Figure 4 presents optical micrographs of PLLA spherulites grown at various cooling rates from 200°C ($> T_m$) to room temperature. Obviously, the size of the PLLA spherulites increases with a decrease in the cooling rate; particularly at slower cooling rates (< 2°C min^{-1}) the PLLA film crystallizes effectively from the isotropic melt with an accompanying annealing treatment. Whenever the PLLA films were cooled at rapid rates (> 20°C min^{-1}) the resultant films became completely amorphous, as confirmed by the X-ray photograph shown in *Figure 5*. The density of these films is almost constant and determined experimentally as 1.256 g cm^{-3}, presumably equal to the 'amorphous density' of PLLA.

As shown in *Figure 6*, a linear relationship seems to hold between exothermic enthalpy change and density for PLLA films. The density change is generally governed by crystallinity of the polymer. Since the crystal density of PLLA (α-form) was estimated[13,18] to be 1.285 g cm^{-3}, the enthalpy of fusion for a large crystal of infinite size corresponds to 135 J g^{-1} as deduced from this relationship. This estimated value is far larger than the 93 J g^{-1} calculated by Fischer *et al.*[20], but more close to value (140 J g^{-1}) of Loomis *et al.*[21].

As described in the preceding section, however, the exothermic enthalpy change obtained by extrapolating the cooling rate to 0°C min^{-1} (see *Figure 2*) is about 60 J g^{-1}. In this case, the maximum crystallinity of the annealed PLLA film is calculated to be almost 0.44. The enthalpy of fusion for the film crystallized at 140°C for 24 h was determined to be 70 J g^{-1}. Therefore, it might be difficult to achieve a degree of crystallinity for PLLA films exceeding the value of about 0.5.

Isothermal crystallization behaviour of PLLA

The spherulite radius of PLLA films measured from optical micrographs is confirmed to change linearly with crystallization time. The spherulite growth rate, G, thus evaluated was 2.0 μm min^{-1} for specimen A ($\overline{M}_w = 2.0 \times 10^5$) at 140°C, similar to that obtained by Pennings and co-workers[6,16] and Tsuji *et al.*[22]. The G values for the specimens of different molecular weight are shown in *Figure 7*. Below 100°C, it was difficult to measure the growth rate because of low segmental mobilities of the PLLA.

Figure 7 shows that the value of G increases with increasing crystallization temperature, T_c; after reaching the maximum, it then decreases with increasing T_c. The crystallization rate increases with decreasing molecular weight of PLLA. The maximum in the rate of spherulite growth is located at about 120°C on the temperature axis. These types of behaviour are very common among ordinary synthetic polymers[23], and are also essentially consistent with those reported by Pennings and co-workers[16].

To characterize the mode of crystallization, the following Avrami equation

$$X_c = 1 - \exp(-kt^n) \tag{1}$$

was applied to the d.l.i. data obtained, where k is the temperature-dependent rate constant and n an integer between 1 and 4 indicating the mode of dimension of crystal growth. $X_c(t)$ represents the fraction of transformed or crystallized material after time t. In the depolarized-light intensity[24,25] technique, it can be expressed as

$$X_c = \frac{I_\infty - I_t}{I_\infty - I_0} \tag{2}$$

where I_∞, I_0 and I_t represent the transmitted-light intensity at very long time, the intensity at initial time and the intensity at an intermediate time, t, respectively.

Avrami theory is useful for determining the mode of crystal growth (spherical, disc-like, etc.) and the overall rate of nucleation-controlled crystallization in polymeric materials. The values of overall crystallization rate, k, from the reciprocal induction period ($1/\tau = k_\tau$) are plotted against T_c in *Figure 8a*. Also, the other k values ($k_{t1/2}$) shown in *Figure 8b* are obtained by use of a fractional conversion of 0.5. Both k values from the different methods increase with increasing T_c; then, after reaching the maximum, decrease with further increase in T_c. These tendencies agree well with that of the spherulite growth rate in *Figure 7*. The maximum in the rate of overall crystallization occurs at a temperature of about 105°C, lower than that (120°C) corresponding to the maximum spherulite growth rate.

Avrami plots of these data for the sample with $\overline{M}_w = 2 \times 10^5$ are shown in *Figure 9*. The average value of n was estimated to be 4 by least-squares fits. Although not shown in the figures, similar values for the Avrami indices were obtained for all PLLA samples of different molecular weight. Thus, the spherulite growth mode of PLLA is three-dimensional with a homogeneous nucleation mode. As shown in *Figure 9*, the n value gradually becomes 3 at longer time scales, since larger spherulites sandwiched between two glass plates have grown into a disc-like shape.

Growth rate parameters in crystallization of PLLA

The kinetic data obtained from *Figure 7* have been examined in terms of secondary nucleation theory[23]. The general expression for the growth rate of a linear polymer crystal with folded chains is given by

$$G = G_0 \exp\left(\frac{-U^*}{R(T_c - T_\infty)}\right) \exp\left(\frac{-K_g}{T_c \Delta T f}\right) \tag{3}$$

where K_g is the nucleation constant; ΔT is the undercooling

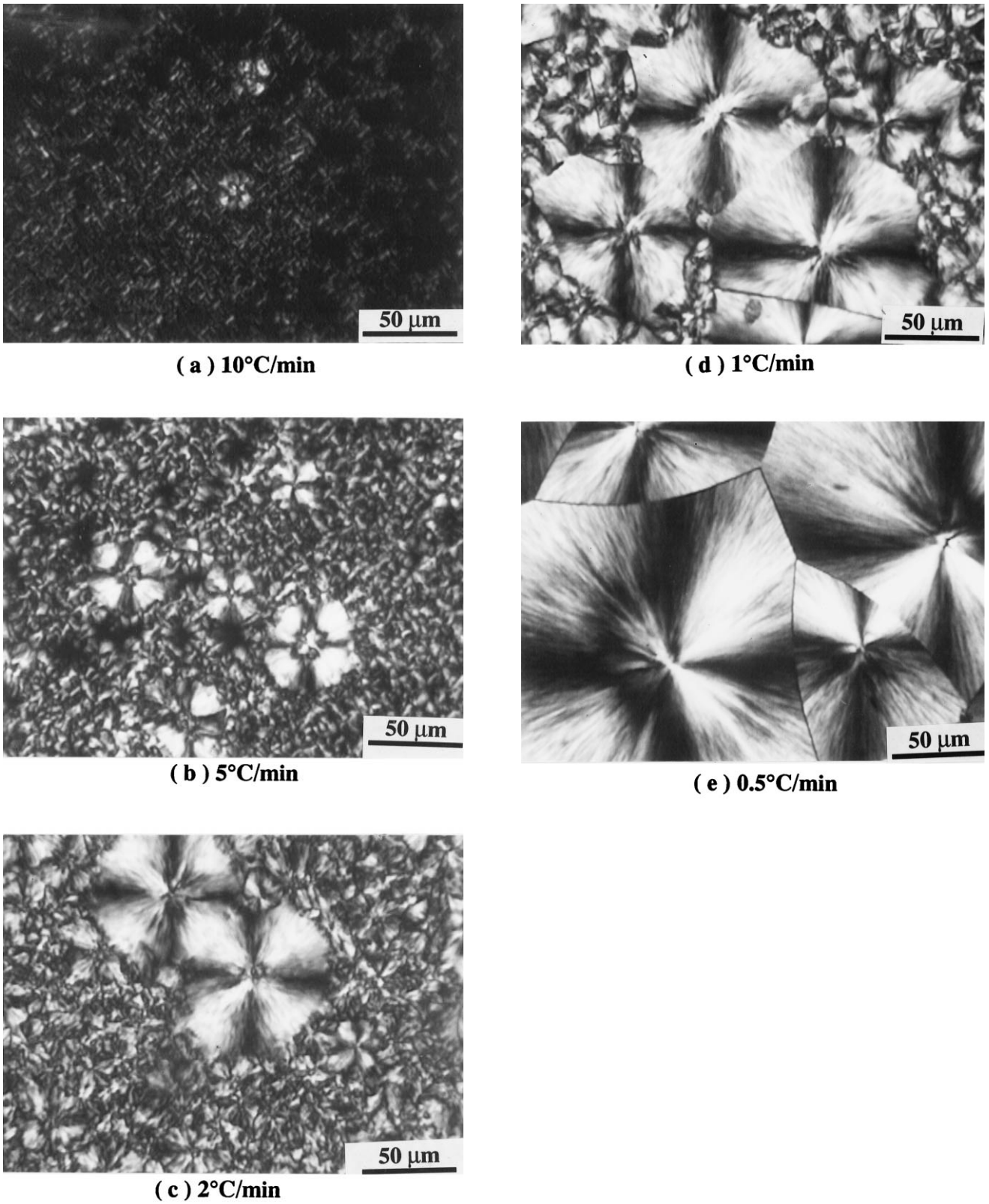

Figure 4 Spherulites of PLLA grown at various cooling rates from the isotropic melt

defined by $T_m^\circ - T_c$; T_m° is the equilibrium melting point; f is a factor given as $2T_c/(T_m^\circ + T_c)$; U^* is the activation energy for segment diffusion to the site of crystallization; R is the gas constant; T_∞ is the hypothetical temperature where all motion associated with viscous flow ceases, $T_g - 50$; and G_0 is the front factor. We apply the equation to our data of PLLA shown in *Figure 7*.

As illustrated in *Figure 10*, log G changes linearly with $1/(T_c - T_\infty)$. These linear relationships give the U^* values from their slopes. *Figure 11* shows plots of $\log G + U^*/2.303R(T - T_\infty)$ versus $1/T_c\Delta Tf$, which give the values of K_g and log G_0 from their slopes and intercepts, respectively. The results obtained from the secondary nucleation analysis are listed in *Table 2*. There is still insufficient direct information on the growth front of PLLA spherulites, since the lamellae structure of PLLA has not yet been examined adequately. When the growth front is assumed to be the (1 1 0) plane of PLLA as in the case of high-density

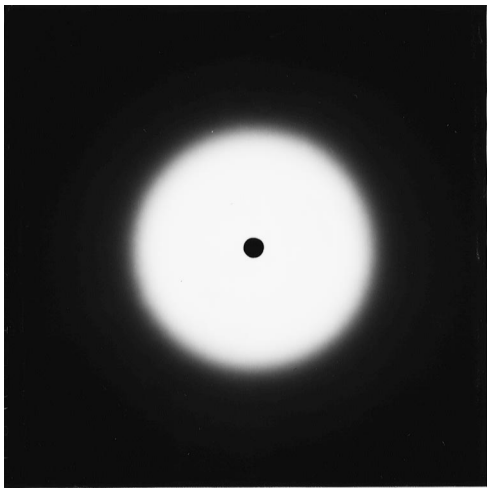

Figure 5 X-ray photograph of the glassy PLLA film obtained with a rapid cooling rate of 20°C min^{-1} from the isotropic melt

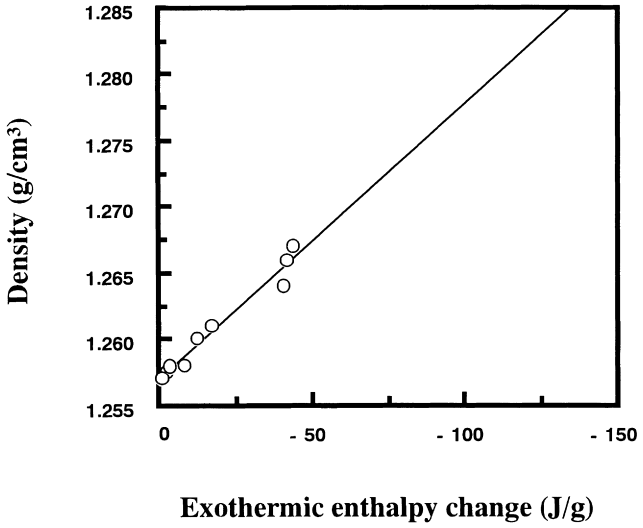

Figure 6 Relationship between exothermic enthalpy change and density for PLLA film specimens

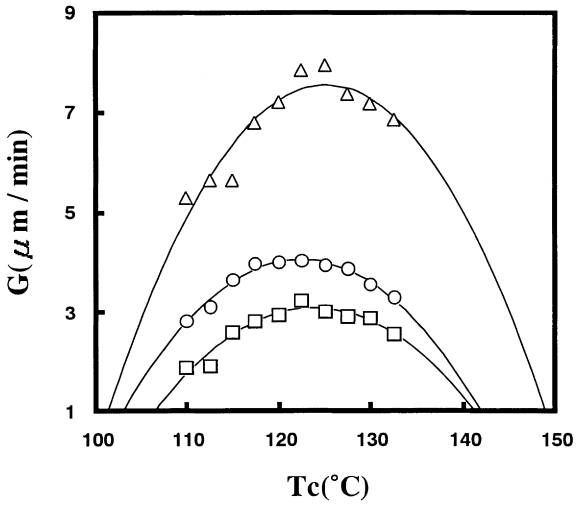

Figure 7 Growth rate G (μm min^{-1}) as a function of isothermal crystallization temperature (T_c) for PLLA films: □, $\overline{M}_w = 2.0 \times 10^5$; ○, $\overline{M}_w = 1.0 \times 10^5$; △, $\overline{M}_w = 5.0 \times 10^4$

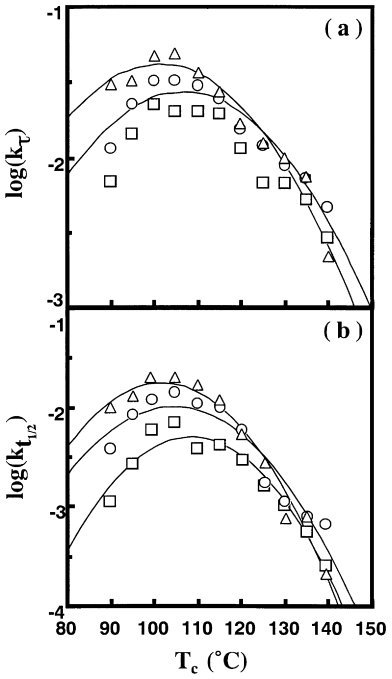

Figure 8 Isothermal overall crystallization rate as a function of crystallization temperature (T_c) for the PLLA films. (a) k_τ is evaluated from the reciprocal induction period; (b) indicates $k_{t1/2}$ obtained at a fractional conversion of 0.5. □, $\overline{M}_w = 2.0 \times 10^5$; ○, $\overline{M}_w = 1.0 \times 10^5$; △, $\overline{M}_w = 5.0 \times 10^4$

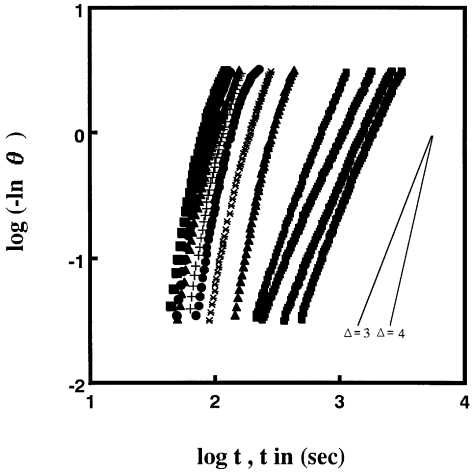

Figure 9 Avrami plots for isothermal crystallization of PLLA films of $\overline{M}_w = 2.0 \times 10^5$ at various T_cs from the isotropic melt at 200°C kept for 5 min. The lines indicate the gradients of 3 and 4

polyethylene, the value of the layer thickness should be taken as 0.53 nm for PLLA crystals[18]. Accordingly, the values of K_g and surface free energies, $\sigma\sigma_e$, can be calculated by considering Regime II growth[23].

The nucleation parameter K_g is given by:

$$K_g = \frac{2b\sigma\sigma_e T_m^\circ}{\Delta h_f k_B} \tag{4}$$

where b is the layer thickness; σ is the lateral surface free energy; σ_e is the fold surface free energy; Δh_f the heat of fusion per unit volume; and k_B Boltzmann's constant.

The values of $\sigma\sigma_e$ estimated are in the range 560–990 $\times$ 10^{-6} J^2 m^{-4}, similar to those found for other polymers[23]. However, these values are slightly larger than Vasanthakumari and Pennings' results[16] for PLLA. It is not clear at present whether or not this difference is caused by the

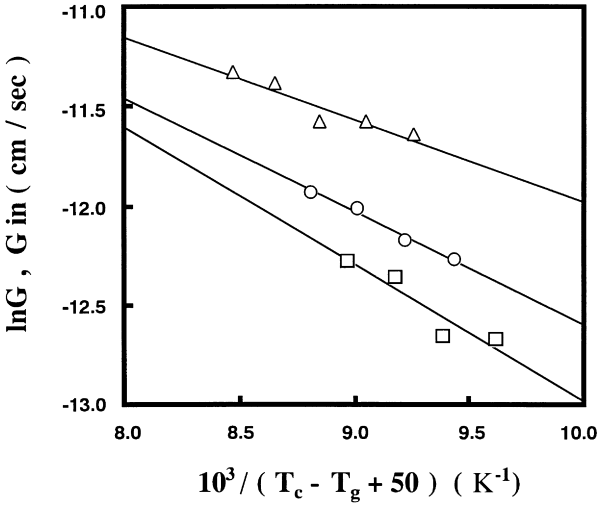

Figure 10 Changes in ln G as a function of $1/(T_c - T_\infty)$. □, $\overline{M}_w = 2.0 \times 10^5$; ○, $\overline{M}_w = 1.0 \times 10^5$; △, $\overline{M}_w = 5.0 \times 10^4$

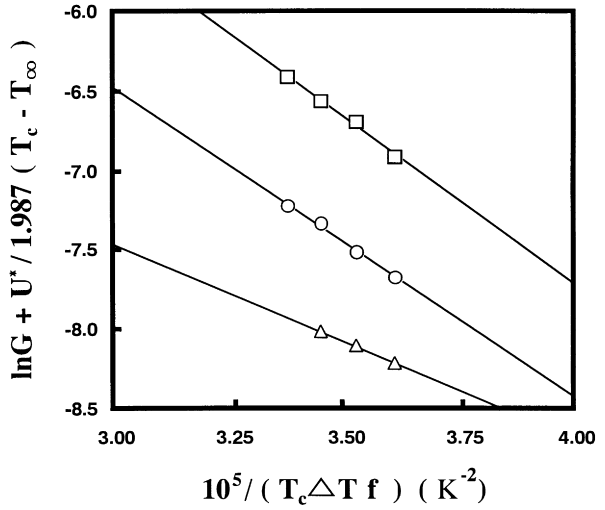

Figure 11 Changes in ln $G + U^*/R(T - T_\infty)$ as a function of $1/T_c\Delta Tf$. □, $\overline{M}_w = 2.0 \times 10^5$; ○, $\overline{M}_w = 1.0 \times 10^5$; △, $\overline{M}_w = 5.0 \times 10^4$

Table 2 Results of the secondary nucleation analysis

$\overline{M}_w$	T_g (°C)	U^* (kJ mol^{-1})	$\sigma\sigma_e$ (J^2 m^{-4})
2.0×10^5	56	5730	991×10^{-6}
1.0×10^5	54	4740	925×10^{-6}
5.0×10^4	52	3427	575×10^{-6}

Parameters used in this analysis

Quantity	Value	Source
Δh_f (J m^{-3})	174×10^6	this work
T_m° (°C)	203	16
d_{110} (m)	5.3×10^{-10}	18

theoretical equation applied. The values of U^* are estimated to range from 3500 to 5700 J mol^{-1}, slightly smaller than those reported for other polymers. Also, these values have a molecular weight dependence.

We then estimated the lateral surface energy, σ, by using the Thomas–Stavely equation[23]

$$\sigma = 0.1 \cdot \Delta h_f \cdot b \quad (5)$$

The σ value was then calculated as 9.2×10^{-3} J m^{-2} for all PLLA samples with different molecular weight. When this value of σ was used to obtain σ_e from their $\sigma\sigma_e$ values estimated above, the σ_e values of specimen A, specimen B and specimen C were 107×10^{-3} J m^{-2}, 100×10^{-3} J m^{-2} and 63×10^{-3} J m^{-2}, respectively. Clearly there seems to be a molecular weight dependence; namely, the value of σ_e increases with increasing molecular weight. This implies that the fold surface of a high-molecular-weight specimen would be predominantly composed of loose-loop folds.

Vasanthakumari and Pennings have reported that Regime I could be applicable to the crystallization data of PLLA since axialite-like morphology is observed[16]. However, we can hardly distinguish the axialite reported by Pennings and co-workers. More detailed examination of the surface morphology of the negatively birefringent PLLA spherulites by electron microscopy and diffraction techniques should be informative concerning the mechanism and mode of spherulite growth.

CONCLUSIONS

The crystallization characteristics of PLLA have been studied by optical microscopy and a depolarized-light intensity method. The results obtained are as follows.

(1) The crystallinity of PLLA depends closely on the cooling rate from its isotropic melt during non-isothermal crystallization.
(2) The overall crystallization rate increases with decreasing molecular weight of PLLA. This behaviour is very similar to that of ordinary synthetic polymers.
(3) The PLLA polymer shows an Avrami exponent $n = 4$ in isothermal crystallization experiments.
(4) Molecular parameters of the crystallization behaviour have been estimated by the application of secondary nucleation theory.

ACKNOWLEDGEMENTS

The authors appreciate the contributions of Mr Kazuo Sasaki of Yamagata University, who carried out some parts of the XRD work and materials arrangements, and Mr Taku Yoshizawa and Miss Rumiko Shimada for their help with the d.l.i. experiments.

REFERENCES

1. Kulkarni, R. K., Moore, E. G., Hegyeli, A. F. and Lenard, F., *J. Biomed. Mater. Res.*, 1971, **5**, 169.
2. Brady, J. M., Cutright, D. E., Miller, R. A., Bottistone, G. C. and Hunsuck, E. E., *J. Biomed. Mater. Res.*, 1973, **7**, 155.
3. Miller, R. A., Brady, J. M. and Cutright, D. E., *J. Biomed. Mater. Res.*, 1977, **11**, 711.
4. Gilding, D. K. and Reed, A. M., *Polymer*, 1979, **20**, 1459.
5. Reed, A. M. and Gilding, D. K., *Polymer*, 1981, **22**, 494.
6. Kalb, B. and Pennings, A. J., *Polymer*, 1980, **21**, 607.
7. Eling, B., Gogolewski, S. and Pennings, A. J., *Polymer*, 1982, **23**, 1587.
8. Zwiers, R. J. M., Gogolewski, S. and Pennings, A. J., *Polymer*, 1983, **24**, 167.
9. Eenink, M. J. D., Feijin, J., Olijslager, J. M., Albers, J. H., Riek, J. C. and Geidanus, P. J., *J. Controlled Release*, 1987, **6**, 225.
10. Kimura, Y., Matsuzaki, Y., Yamane, H. and Kitao, T., *Polymer*, 1989, **30**, 1342.
11. Reeve, M. S., McCarthy, S. P., Downey, M. J. and Gross, R. A., *Macromolecules*, 1994, **27**, 825.
12. De Santis, P. and Kovacs, A. J., *Biopolymers*, 1968, **6**, 299.

13. Hoogsteen, W., Postema, A. R., Pennings, A. J., tenBrinke, G. and Zugenmaier, P., *Macromolecules*, 1990, **23**, 634.
14. Kobayashi, J., Asahi, T., Ichiki, M., Okikawa, A., Suzuki, H., Watanabe, T., Fukada, E. and Shikinami, Y., *J. Appl. Phys.*, 1995, **77**, 2957.
15. Brizzolara, D., Cantow, H. J., Diederichs, K., Keller, E. and Domb, A. J., *Macromolecules*, 1996, **29**, 191.
16. Vasanthakumari, R. and Pennings, A. J., *Polymer*, 1983, **24**, 175.
17. Kishore, K. and Vasanthakumari, R., *Colloid Polym. Sci.*, 1988, **266**, 999.
18. Miyata, T. and Masuko, T., *Polymer*, 1997, **38**, 4003.
19. Masuko, T., Okuizumi, R., Yonetake, K. and Magill, J. H., *Macromolecules*, 1989, **22**, 4636.
20. Fischer, E. W., Sterzel, H. J. and Wegner, G., *Kolloid-Z. u.Z. Polymere*, 1973, **251**, 980.
21. Loomis, G. L., Mudoch, J. R. and Gardner, K. H., *Polym. Prepr. (Am. Chem. Soc., Div. Polym. Chem.)*, 1990, **31**, 55.
22. Tsuji, H. and Ikada, Y., *Polymer*, 1995, **36**, 2709.
23. Hoffman, J. D., Davis, G. T. and Lauritzen, J. I., *Treatise on Solid State Chemistry*, vol. 3, ed. N. B. Hannay. Plenum, New York, 1976.
24. Magill, J. H., *Nature*, 1960, **187**, 771.
25. Magill, J. H., *Nature*, 1961, **191**, 1092.